Ultrathin Bacterial Cellulose Membrane with Voronoi-nets Structure for Low Pressure and High Flux Microfiltration

Ning Tang,[a] Shichao Zhang,[b] Yang Si,[a,b]* Jianyong Yu,[a,b] and Bin Ding[a,b]*

[a] State Key Laboratory for Modification of Chemical Fibers and Polymer Materials, College of Textiles, Donghua University, Shanghai 201620, China

[b] Innovation Center for Textile Science and Technology, Donghua University, Shanghai 200051, China

Supplementary Information contains:

Supplementary Fig. S1−S13

Supplementary Table 1

Supplementary Discussions

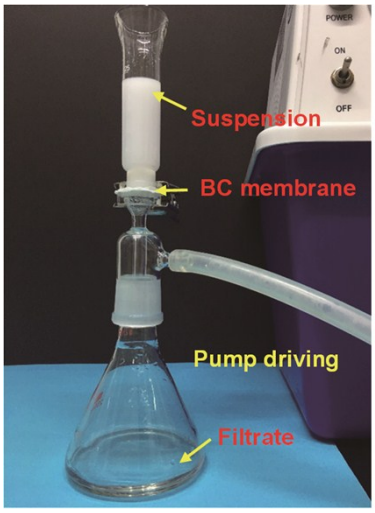

Fig. S1 Digital photo of the dead-end filtration system.

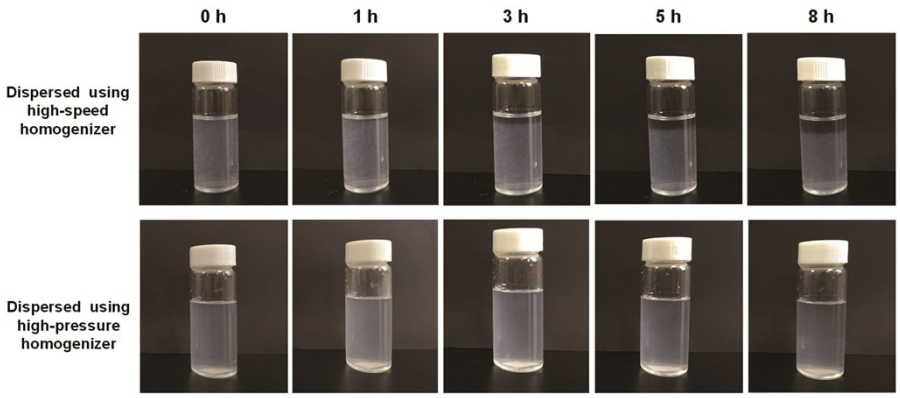

Fig. S2 Effect of dispersed methods on the stability of BC dispersion.

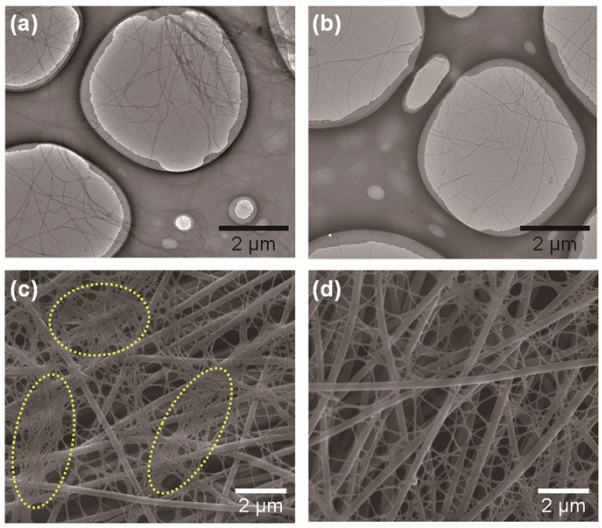

Fig. S3 TEM images of the BC nanofibers obtained by (a) high-speed homogenization, and (b) high-pressure homogenization. SEM images of BC membranes obtained from (c) high-speed homogenized BC nanofibers, and (d) high-pressure homogenized BC nanofibers. (PAN15 as the substrate, BC loading content of 40 mg m^{-2}).

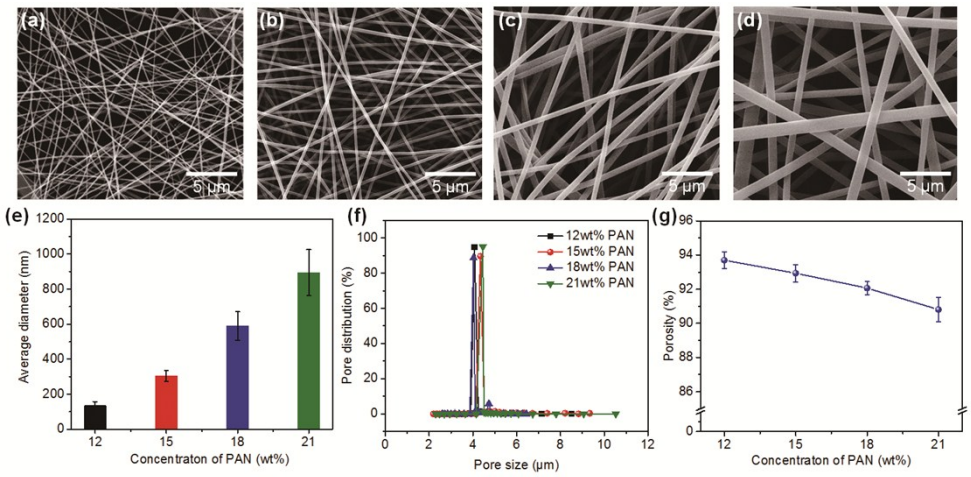

Fig. S4 SEM images of electrospun PAN NMs prepared from solutions with different concentrations of (a) 12, (b) 15, (c) 18, (d) 21 wt%. (e) Average diameter, (f) pore size distribution, and (g) porosity of the corresponding nanofibrous membranes.

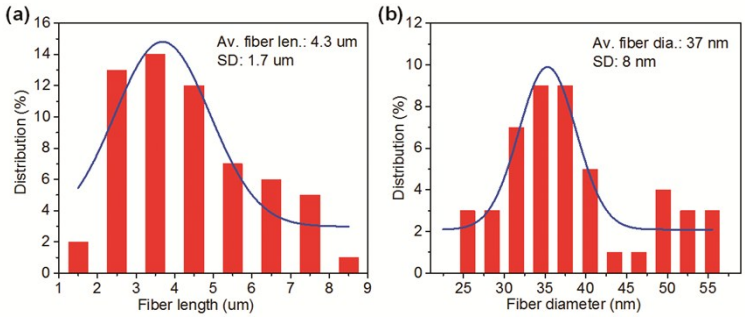

Fig. S5 (a) Fiber length and (b) fiber diameter distribution of the BC nanofibers in dispersion.

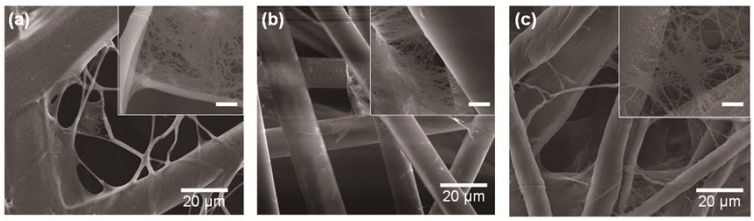

Fig. S6 SEM images of BC membranes with substrate of (a) hydrophilic melt-blown non-woven fabric, (b) hydrophilic spun-bonded non-woven fabric, (c) cellulose filter paper (BC loading content of 40 mg m^{-2}. Scale bar in the insets is 2 μm.)

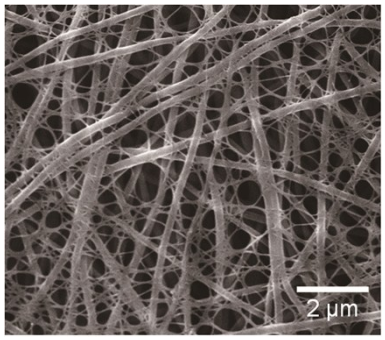

Fig. S7 SEM image of BC membrane before cross-linking (PAN15-BC40 as an example).

Table S1. TOC content in pure water and soaking solution of different membranes.

Samples	TOC content (mg L^{-1})
Pure water	0.45 ± 0.15
PAN15	0.74 ± 0.21
PAN15-BC40	1.76 ± 0.21
c-PAN15-BC40	0.71 ± 0.03

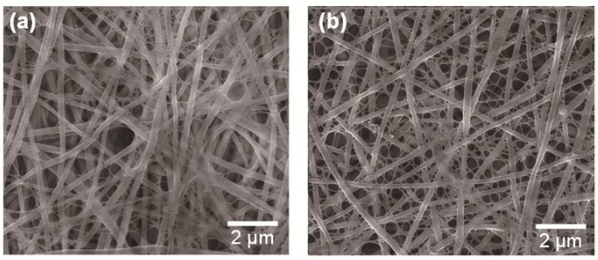

Fig. S8 SEM images of (a) PAN15-BC40 and (b) c-PAN15-BC40 after soaked in pure water and vortexed for 10 min.

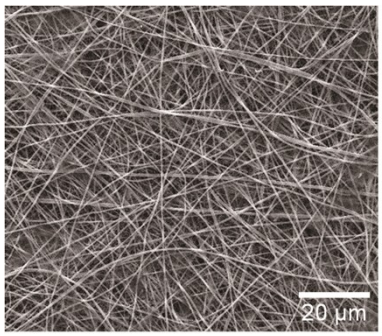

Fig. S9 SEM image of c-PAN15-BC40 with low magnification.

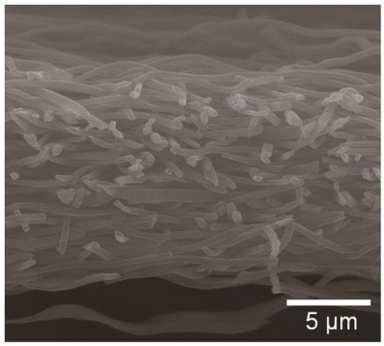

Fig. S10 Cross-sectional SEM image of PAN15.

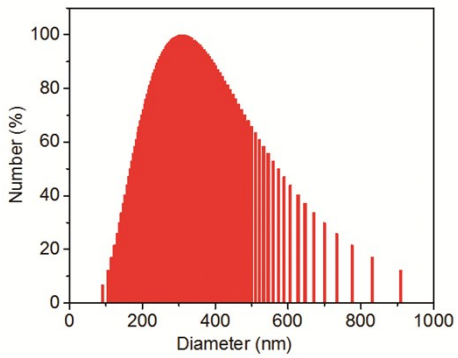

Fig. S11 The dynamic light scattering size distribution of TiO_2 microparticles in the feed solution.

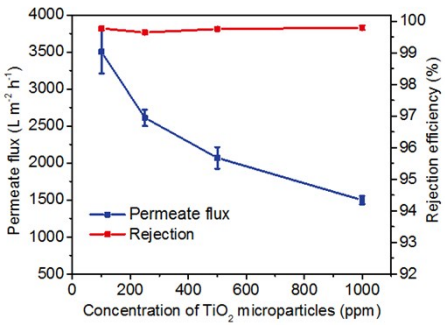

Fig. S12 Permeate fluxes and rejection efficiencies of c-PAN15-BC90 for different concentration of TiO_2 microparticles under the driving force of 5kPa.

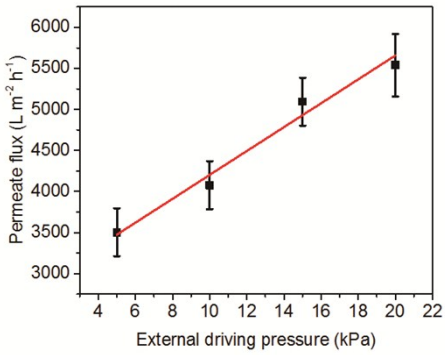

Fig. S13 Fitted curve between permeate flux and external driving pressure ranging from 5 to 20 kPa.

Supplementary Discussions

Optimization of the BC nanofibres dispersion

The condition of fiber dispersion is one of the vital factors on the structure construction of Voronoi-like nanonets. To ensure the uniformity of nanonets, BC nanofibers dispersion must stable. Fig. S2 shows the effect of dispersed methods on the stability of BC nanofibers dispersion. It can be seen that, BC nanofibers dispersion obtained by high-speed homogenization became nonuniform after setting 3 h. Whereas, BC nanofibers dispersion obtained via high-pressure homogenization was still uniform and stable even after 8 h. Meanwhile, compared with BC nanofibers obtained by high-speed homogenization, which showed more entanglement, BC nanofibers obtained by high-pressure homogenization were demonstrated more homogeneous, resulting in the corresponding BC membrane with uniform Voronoi-like nanonets (Fig. S3).